Mueller matrix analysis for all optical fiber co-existence of birefringence-polarization dependent gain-mode coupling at a single wavelength*

Shang Chao(尚 超), Wu Chong-Qing(吴重庆)†, Li Zheng-Yong(李政勇), Yang Shuang-Shou(杨双收), Gao Kai-Qiang(高凯强), Yu Kuang-Lu(余贶琭), and Feng Zhen(冯 震)

Key Laboratory of Education Ministry on Luminescence and Optical Information Technology, Institute of Optical Information, Beijing Jiaotong University, Beijing 100044, *China*

(Received 14 January 2011; revised manuscript received 5 May 2011)

Birefringence (polarization-related phase-shift), polarization dependent gain (PDG) and mode coupling are three factors that may synchronously influence the transmission of single-wavelength polarized light in optical fibers. This paper obtains a new Mueller matrix analysis, which can be used under conditions that all these three factors are existing and changing. According to our transmission model, the state of polarization (SOP) changes along an optical microstructure fiber with co-existence of birefringence-PDG-mode coupling were simulated. The simulated results, which show the phenomena of SOP constringency, are in good agreement with previous theoretical analyses.

Keywords: Mueller matrix, birefringence, polarization dependent gain, mode coupling

PACS: 02.10.Yn, 42.81.–i **DOI:** 10.1088/1674-1056/20/11/110201

1. Introduction

With the progresses of optical communication systems, research on the state of polarization (SOP) control technologies becomes increasingly important. Those technologies can be used in various fields, such as the PMD (polarization mode dispersion) compensation,[1−3] coherent optical communication,[4,5] polarization based optical code division multiple access (OCDMA),[6,7] polarization multiplexing in optical time domain multiplexing (OTDM)[8] and design of microstructure optical fibers.[9] Any polarized light's SOP can be completely described by four measurable quantities now known as the Stokes polarization parameters $\boldsymbol{S}$,[10] and Mueller calculus is a matrix-algebraic method of specifying a beam of light and the optical devices encountered by the beam, and computing the SOP of output light,[11] where $\boldsymbol{S}_{\rm out} = \boldsymbol{M}\boldsymbol{S}_{\rm in}$, where $\boldsymbol{M}$ is a 4×4 Mueller matrix.

Birefringence, PDG and mode coupling exist universally in fibers. Firstly, the birefringence is one of the basic polarization effects which contribute to the well-known PMD.[12] Secondly, the possible PDG or polarization dependent loss (PDL) occurs when a fiber is bent or in some special optical fibers as non-circular air holes microstructure optical fibers (MOFs), poled fibers, fiber polarizers and liquid crystal cladding fibers. Thirdly, extensive mode coupling occurs in twisted fibers, span fibers, connectors, splices and other passive components in an optical link.[13]

Sometimes, not all of the three factors play major roles in some kinds of fibers, so only one or two factors need to be considered to find the SOP changes. In these conditions, many papers are devoted to the Mueller matrix theoretical analyses. The Mueller matrix method in a fiber system with both birefringence and PDL factors have been proposed,[14,15] and the matrix considering both birefringence and mode coupling has also been given.[16]

In some conditions, however, the birefringence, PDG and mode coupling should be considered at the same time in some optical transmission mediums, such as research and design of the hyperfine SOP evolvement for some MOFs. Unfortunately, no appropriate Mueller matrix analysis with the co-existence of birefringence-PDG-mode coupling has been put forward. An accurate and elaborate Mueller matrix model is the foundation for studying the SOP problems in optical systems. Therefore, new Mueller ma-

*Project supported by the National Natural Science Foundation of China (Grants Nos. 60877057 and 60907027).

†Corresponding author. E-mail: cqwu@bjtu.edu.cn

© 2011 Chinese Physical Society and IOP Publishing Ltd

trix analyses for the above situations would be beneficial for research and development of high speed and optical communication devices.

In this paper, a new Mueller matrix analysis is proposed and the derivative processes of a single wavelength Mueller matrix with co-existence of birefringence-PDG-mode coupling are given in detail. At first, a mode coupling matrix considering all three factors is proposed in Section 2, then the Jones matrix is obtained from the mode coupling matrix, and the Mueller matrix is calculated from the Jones matrix in Section 3. In Section 4, the simulation results are given and some SOP constringency phenomena are obtained, which can prove the correctness of the new Mueller matrix analysis.

2. The mode coupling equation for co-existence of birefringence-PDG-mode coupling

Although the mode coupling equation with birefringence is well-known,[17] it is not appropriate when considering two orthogonal modes with PDG/PDL. Thus, a new mode coupling equation with the PDG/PDL should be deduced. Set the principal x_0–y_0 axis of PDG/PDL in the first Δz segment of fiber to coincide with the x–y axis, then the axis of PDG/PDL in the next segment after mode coupling would not be affected, Fig. 1 is the schematic diagram. The coordinate system for birefringence is the same as the one for PDG/PDL.

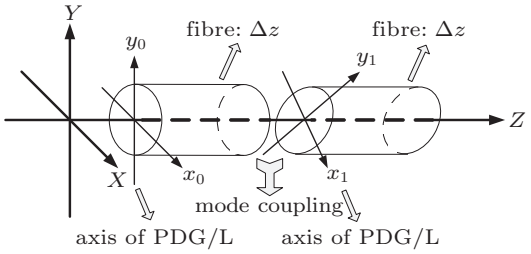


Fig. 1. Axis x–y of PDG/PDL in an optical fiber.

The optical field propagates along the z-axis and the transverse components of the optical fields are represented by

$$\boldsymbol{E} = \begin{bmatrix} \dot{E}_x(z) \\ \dot{E}_y(z) \end{bmatrix} = \begin{bmatrix} \dot{E}_{x0}(z)\,\mathrm{e}^{-\alpha_x z} \\ \dot{E}_{y0}(z)\,\mathrm{e}^{-\alpha_y z} \end{bmatrix}, \tag{1}$$

where α_x and α_y are the transmission loss coefficients (real number) along the z direction, $\dot{E}_{x0}$ and $\dot{E}_{y0}$ are the two components of Jones vectors in lossless condition. According to mode coupling theory, the mode coupling equations and its matrix $\boldsymbol{C}_{\mathrm{int}}$ under co-existence of birefringence-PDG-mode coupling condition can be described as

$$\begin{cases} \dfrac{\mathrm{d}\dot{E}_x}{\mathrm{d}z} = c_{11}\dot{E}_x + c_{12}\dot{E}_y, \\ \dfrac{\mathrm{d}\dot{E}_y}{\mathrm{d}z} = c_{21}\dot{E}_x + c_{22}\dot{E}_y, \end{cases} \quad \boldsymbol{C}_{\mathrm{int}} = \begin{bmatrix} c_{11} & c_{12} \\ c_{21} & c_{22} \end{bmatrix}. \tag{2}$$

Because of the symmetry of mode coupling, c_{12} is equal to c_{21}. Substitute $\dot{E}_{x0}$ and $\dot{E}_{y0}$ in Eq. (1) into $\dot{E}_x$ and $\dot{E}_y$ in Eq. (2), then a new mode coupling equation can be expressed as

$$\begin{cases} \dfrac{\mathrm{d}\dot{E}_{x0}}{\mathrm{d}z} = (c_{11} + \alpha_x)\,\dot{E}_{x0} + c_{12}\dot{E}_{y0}\,\mathrm{e}^{(\alpha_x - \alpha_y)z}, \\ \dfrac{\mathrm{d}\dot{E}_{y0}}{\mathrm{d}z} = c_{21}\dot{E}_{x0}\,\mathrm{e}^{-(\alpha_x - \alpha_y)z} + (c_{22} + \alpha_y)\,\dot{E}_{y0}. \end{cases} \tag{3}$$

Based on the energy conservation law, the total energy of $\dot{E}_{x0}$ and $\dot{E}_{y0}$ is a constant under lossless condition, that is

$$\frac{\mathrm{d}}{\mathrm{d}z}\left\{\left|\dot{E}_{x0}\right|^2 + \left|\dot{E}_{y0}\right|^2\right\} = \frac{\mathrm{d}}{\mathrm{d}z}\left\{\dot{E}_{x0}\dot{E}^*_{x0} + \dot{E}_{y0}\dot{E}^*_{y0}\right\} \equiv 0. \tag{4}$$

Substituting Eq. (3) into Eq. (4), we obtain

$$\begin{aligned} &(c_{11} + c^*_{11} + 2\alpha_x)\,\dot{E}_{x0}\dot{E}^*_{x0} + (c_{12} \\ &\quad + c^*_{21})\dot{E}_{y0}\dot{E}^*_{x0}\,\mathrm{e}^{-(\alpha_x - \alpha_y)z} \\ &\quad + (c^*_{12} + c_{21})\,\dot{E}_{x0}\dot{E}^*_{y0}\,\mathrm{e}^{-(\alpha_x - \alpha_y)z} \\ &\quad + (c^*_{22} + c_{22} + 2\alpha_y)\,\dot{E}_{y0}\dot{E}^*_{y0} \equiv 0. \end{aligned} \tag{5}$$

If Eq. (5) holds true under any condition, the coefficients must satisfy

$$\begin{cases} c_{11} + c^*_{11} + 2\alpha_x = 0, \\ c_{22} + c^*_{22} + 2\alpha_y = 0, \\ c_{12} = -c^*_{21}. \end{cases} \tag{6}$$

The coefficients c_{11} and c_{22} can be divided into the real parts and the imaginary parts, namely $c_{11} = c_{11\mathrm{r}} + \mathrm{i}c_{11\mathrm{i}}$, and $c_{22} = c_{22\mathrm{r}} + \mathrm{i}c_{22\mathrm{i}}$. Hence, from Eq. (6) we have $2c_{11\mathrm{r}} + 2\alpha_x = 0$, $2c_{22\mathrm{r}} + 2\alpha_y = 0$, where $c_{11\mathrm{i}}$ and $c_{22\mathrm{i}}$ are the self-coupling coefficients, in other words, they are the propagation constants β_x and β_y in noncircular regular optical fibers. Note also that $c_{12} = c_{21} \neq 0$, which means that c_{12} and c_{21} are pure imaginary numbers, so they can be written as

$c_{12} = c_{21} = \mathrm{i}k$, where k is the mode coupling coefficient (a real number). Then a new mode coupling matrix for co-existence of birefringence-PDG-mode coupling condition can be written as

$$\boldsymbol{C} = \begin{bmatrix} -\alpha_x + \mathrm{i}\beta_x & \mathrm{i}k \\ \mathrm{i}k & -\alpha_y + \mathrm{i}\beta_y \end{bmatrix}. \tag{7}$$

Considering the PDG, we can set g_x and g_y as the gain coefficients, instead of $-\alpha_x$ and $-\alpha_y$, we can write the new mode coupling matrix $\boldsymbol{C}$ as

$$\boldsymbol{C} = \begin{bmatrix} g_x + \mathrm{i}\beta_x & \mathrm{i}k \\ \mathrm{i}k & g_y + \mathrm{i}\beta_y \end{bmatrix}. \tag{8}$$

According to Eq. (8), the mode coupling equations (2) is changed to

$$\begin{cases} \dfrac{\mathrm{d}\dot{E}_{x0}}{\mathrm{d}z} = (g_x + \mathrm{i}\beta_x)\dot{E}_{x0} + \mathrm{i}k\dot{E}_{y0}, \\ \dfrac{\mathrm{d}\dot{E}_{y0}}{\mathrm{d}z} = \mathrm{i}k\dot{E}_{x0} + (g_y + \mathrm{i}\beta_y)\dot{E}_{y0}. \end{cases} \tag{9}$$

If matrix $\boldsymbol{C}$ is independent of z, and the coefficients g_x, g_y, β_x, β_y and k are all real numbers, Eq. (9) can be regarded as liner differential equations with constant coefficients, and the light fields can be solved as

$$\begin{bmatrix} \dot{E}_x(z) \\ \dot{E}_y(z) \end{bmatrix} = \exp\left[(g + \mathrm{i}\,\beta)\, z\right] \begin{bmatrix} \cos(-\mathrm{i}\,\eta z) + \dfrac{\mathrm{i}\,\Delta g - \Delta\beta}{\eta}\sin(-\mathrm{i}\,\eta z) & -\dfrac{k}{\eta}\sin(-\mathrm{i}\,\eta z) \\ -\dfrac{k}{\eta}\sin(-\mathrm{i}\,\eta z) & \cos(-\mathrm{i}\,\eta z) - \dfrac{\mathrm{i}\,\Delta g - \Delta\beta}{\eta}\sin(-\mathrm{i}\,\eta z) \end{bmatrix} \begin{bmatrix} \dot{E}_x(0) \\ \dot{E}_y(0) \end{bmatrix}. \tag{10}$$

The parameters g, Δg, β, $\Delta\beta$ and η are defined as below, respectively:

$$g = \frac{g_x + g_y}{2}, \quad \Delta g = \frac{g_x - g_y}{2}, \quad \beta = \frac{\beta_x + \beta_y}{2}, \quad \Delta\beta = \frac{\beta_x - \beta_y}{2}, \quad \eta = \sqrt{(\Delta g - \mathrm{i}\,\Delta\beta)^2 - k^2}. \tag{11}$$

3. The Mueller matrix analysis

Equation (9) can be used to calculate the new Mueller matrix. Equation (12) is the relationship between the Jones complex vector $\boldsymbol{E} = \left[\dot{E}_x(z)\ \dot{E}_y(z)\right]^{\mathrm{T}}$ and its corresponding Stokes vector $\boldsymbol{S}$.

$$\boldsymbol{S} = \begin{bmatrix} s_0 \\ s_1 \\ s_2 \\ s_3 \end{bmatrix} = \begin{bmatrix} \boldsymbol{E}^+ A_0 \boldsymbol{E} \\ \boldsymbol{E}^+ A_1 \boldsymbol{E} \\ \boldsymbol{E}^+ A_2 \boldsymbol{E} \\ \boldsymbol{E}^+ A_3 \boldsymbol{E} \end{bmatrix}, \tag{12}$$

where A_j $(j = 1, 2, 3)$ are Pauli matrices, and they are

$$\boldsymbol{A}_0 = \begin{bmatrix} 1 & 0 \\ 0 & 1 \end{bmatrix}, \quad \boldsymbol{A}_1 = \begin{bmatrix} 1 & 0 \\ 0 & -1 \end{bmatrix}, \quad \boldsymbol{A}_2 = \begin{bmatrix} 0 & 1 \\ 1 & 0 \end{bmatrix}, \quad \boldsymbol{A}_3 = \begin{bmatrix} 0 & \mathrm{i} \\ -\mathrm{i} & 0 \end{bmatrix}, \tag{13}$$

and the symbol '+' means Hermite transposition ($\boldsymbol{U}^+ = \boldsymbol{U}^{*T}$). Substituting $\boldsymbol{E}$, $\boldsymbol{E}^+$ and A_j $(j = 1, 2, 3)$ into Eq. (12), we can calculate s_0, s_1, s_2 and s_3 respectively. Finally, a new Mueller matrix $\boldsymbol{M}$ is obtained as follows:

$$\boldsymbol{M} = \mathrm{e}^{2gz} \begin{bmatrix} \left(\dfrac{\eta_{\mathrm{i}}^2 - \Delta\beta^2 - k^2}{\eta_{\mathrm{r}}^2 + \eta_{\mathrm{i}}^2}\right)\cos(2\eta_{\mathrm{i}} z) & \left(\dfrac{\Delta g\eta_{\mathrm{r}} + \Delta\beta\eta_{\mathrm{i}}}{\eta_{\mathrm{r}}^2 + \eta_{\mathrm{i}}^2}\right)\sinh(2\eta_{\mathrm{r}} z) & \dfrac{k\eta_{\mathrm{i}}}{\eta_{\mathrm{r}}^2 + \eta_{\mathrm{i}}^2}\sinh(2\eta_{\mathrm{r}} z) & \dfrac{k\Delta g}{\eta_{\mathrm{r}}^2 + \eta_{\mathrm{i}}^2}\cosh(2\eta_{\mathrm{r}} z) \\ +\left(\dfrac{\eta_{\mathrm{i}}^2 + \Delta g^2}{\eta_{\mathrm{r}}^2 + \eta_{\mathrm{i}}^2}\right)\cosh(2\eta_{\mathrm{r}} z) & +\left(\dfrac{\Delta g\eta_{\mathrm{i}} - \Delta\beta\eta_{\mathrm{r}}}{\eta_{\mathrm{r}}^2 + \eta_{\mathrm{i}}^2}\right)\sin(2\eta_{\mathrm{i}} z) & -\dfrac{k\eta_{\mathrm{r}}}{\eta_{\mathrm{r}}^2 + \eta_{\mathrm{i}}^2}\sin(2\eta_{\mathrm{i}} z) & -\dfrac{k\Delta g}{\eta_{\mathrm{r}}^2 + \eta_{\mathrm{i}}^2}\cos(2\eta_{\mathrm{i}} z) \\ \left(\dfrac{\Delta g\eta_{\mathrm{r}} + \Delta\beta\eta_{\mathrm{i}}}{\eta_{\mathrm{r}}^2 + \eta_{\mathrm{i}}^2}\right)\sinh(2\eta_{\mathrm{r}} z) & \left(\dfrac{\eta_{\mathrm{i}}^2 - \Delta\beta^2}{\eta_{\mathrm{r}}^2 + \eta_{\mathrm{i}}^2}\right)\cos(2\eta_{\mathrm{i}} z) & \dfrac{k\Delta\beta}{\eta_{\mathrm{r}}^2 + \eta_{\mathrm{i}}^2}\cosh(2\eta_{\mathrm{r}} z) & \dfrac{k\eta_{\mathrm{r}}}{\eta_{\mathrm{r}}^2 + \eta_{\mathrm{i}}^2}\sinh(2\eta_{\mathrm{r}} z) \\ +\left(\dfrac{\Delta g\eta_{\mathrm{i}} - \Delta\beta\eta_{\mathrm{r}}}{\eta_{\mathrm{r}}^2 + \eta_{\mathrm{i}}^2}\right)\sin(2\eta_{\mathrm{i}} z) & +\left(\dfrac{\eta_{\mathrm{i}}^2 + \Delta g^2 - k^2}{\eta_{\mathrm{r}}^2 + \eta_{\mathrm{i}}^2}\right)\cosh(2\eta_{\mathrm{r}} z) & -\dfrac{k\Delta\beta}{\eta_{\mathrm{r}}^2 + \eta_{\mathrm{i}}^2}\cos(2\eta_{\mathrm{i}} z) & +\dfrac{k\eta_{\mathrm{i}}}{\eta_{\mathrm{r}}^2 + \eta_{\mathrm{i}}^2}\sin(2\eta_{\mathrm{i}} z) \\ \dfrac{k\eta_{\mathrm{i}}}{\eta_{\mathrm{r}}^2 + \eta_{\mathrm{i}}^2}\sinh(2\eta_{\mathrm{r}} z) & \dfrac{k\Delta\beta}{\eta_{\mathrm{r}}^2 + \eta_{\mathrm{i}}^2}\cosh(2\eta_{\mathrm{r}} z) & \left(\dfrac{\eta_{\mathrm{i}}^2 + \Delta g^2 - k^2}{\eta_{\mathrm{r}}^2 + \eta_{\mathrm{i}}^2}\right)\cos(2\eta_{\mathrm{i}} z) & -\left(\dfrac{\Delta g\eta_{\mathrm{i}} - \Delta\beta\eta_{\mathrm{r}}}{\eta_{\mathrm{r}}^2 + \eta_{\mathrm{i}}^2}\right)\sinh(2\eta_{\mathrm{r}} z) \\ -\dfrac{k\eta_{\mathrm{r}}}{\eta_{\mathrm{r}}^2 + \eta_{\mathrm{i}}^2}\sin(2\eta_{\mathrm{i}} z) & -\dfrac{k\Delta\beta}{\eta_{\mathrm{r}}^2 + \eta_{\mathrm{i}}^2}\cos(2\eta_{\mathrm{i}} z) & +\left(\dfrac{\eta_{\mathrm{i}}^2 - \Delta\beta^2}{\eta_{\mathrm{r}}^2 + \eta_{\mathrm{i}}^2}\right)\cosh(2\eta_{\mathrm{r}} z) & +\left(\dfrac{\Delta g\eta_{\mathrm{r}} + \Delta\beta\eta_{\mathrm{i}}}{\eta_{\mathrm{r}}^2 + \eta_{\mathrm{i}}^2}\right)\sin(2\eta_{\mathrm{i}} z) \\ \dfrac{k\Delta g}{\eta_{\mathrm{r}}^2 + \eta_{\mathrm{i}}^2}\cos(2\eta_{\mathrm{i}} z) & -\dfrac{k\eta_{\mathrm{r}}}{\eta_{\mathrm{r}}^2 + \eta_{\mathrm{i}}^2}\sinh(2\eta_{\mathrm{r}} z) & \left(\dfrac{\Delta g\eta_{\mathrm{i}} - \Delta\beta\eta_{\mathrm{r}}}{\eta_{\mathrm{r}}^2 + \eta_{\mathrm{i}}^2}\right)\sinh(2\eta_{\mathrm{r}} z) & \left(\dfrac{\eta_{\mathrm{i}}^2 + \Delta g^2}{\eta_{\mathrm{r}}^2 + \eta_{\mathrm{i}}^2}\right)\cos(2\eta_{\mathrm{i}} z) \\ -\dfrac{k\Delta g}{\eta_{\mathrm{r}}^2 + \eta_{\mathrm{i}}^2}\cosh(2\eta_{\mathrm{r}} z) & -\dfrac{k\eta_{\mathrm{i}}}{\eta_{\mathrm{r}}^2 + \eta_{\mathrm{i}}^2}\sin(2\eta_{\mathrm{i}} z) & -\left(\dfrac{\Delta g\eta_{\mathrm{r}} + \Delta\beta\eta_{\mathrm{i}}}{\eta_{\mathrm{r}}^2 + \eta_{\mathrm{i}}^2}\right)\sin(2\eta_{\mathrm{i}} z) & +\left(\dfrac{\eta_{\mathrm{i}}^2 - \Delta\beta^2 - k^2}{\eta_{\mathrm{r}}^2 + \eta_{\mathrm{i}}^2}\right)\cosh(2\eta_{\mathrm{r}} z) \end{bmatrix}. \tag{14}$$

It is easy to see that some parts of matrix $\boldsymbol{M}$ are symmetric and other parts are antisymmetric. When we consider the especial condition, namely z tends to infinity and the other parameters are fixed, the expression of $\boldsymbol{M}$ turns into Eq. (15).

$$\boldsymbol{M} = \frac{\mathrm{e}^{2\alpha z + 2\eta_{\mathrm{r}} z}}{2\left(\eta_{\mathrm{r}}^2 + \eta_{\mathrm{i}}^2\right)} \begin{bmatrix} \eta_{\mathrm{i}}^2 + \Delta\alpha^2 & \Delta\alpha\eta_{\mathrm{r}} + \Delta\beta\eta_{\mathrm{i}} & k\eta_{\mathrm{i}} & k\Delta\alpha \\ \Delta\alpha\eta_{\mathrm{r}} + \Delta\beta\eta_{\mathrm{i}} & \eta_{\mathrm{i}}^2 + \Delta\alpha^2 - k^2 & k\Delta\beta & k\eta_{\mathrm{r}} \\ k\eta_{\mathrm{i}} & k\Delta\beta & \eta_{\mathrm{i}}^2 - \Delta\beta^2 & -\left(\Delta\alpha\eta_{\mathrm{i}} - \Delta\beta\eta_{\mathrm{r}}\right) \\ -k\Delta\alpha & -k\eta_{\mathrm{r}} & \Delta\alpha\eta_{\mathrm{i}} - \Delta\beta\eta_{\mathrm{r}} & \eta_{\mathrm{i}}^2 - \Delta\beta^2 - k^2 \end{bmatrix}. \tag{15}$$

The new coefficients are defined by

$$\begin{cases} \eta = \eta_{\mathrm{r}} + \mathrm{i}\,\eta_{\mathrm{i}}, \\ \eta^* = \eta_{\mathrm{r}} - \mathrm{i}\,\eta_{\mathrm{i}}, \\ \eta\eta^* = \eta_{\mathrm{r}}^2 + \eta_{\mathrm{i}}^2, \\ \eta_{\mathrm{r}}\eta_{\mathrm{i}} = -\Delta\alpha\Delta\beta, \\ \eta_{\mathrm{r}}^2 = \Delta\alpha^2 - \Delta\beta^2 - k^2 + \eta_{\mathrm{i}}^2. \end{cases} \tag{16}$$

4. Simulation

We can use the new Mueller matrix analysis to investigate the SOP evolvement in a special optical fiber, such as an MOF with elliptical air holes whose cross sectional schematic diagram is shown in Fig. 2.

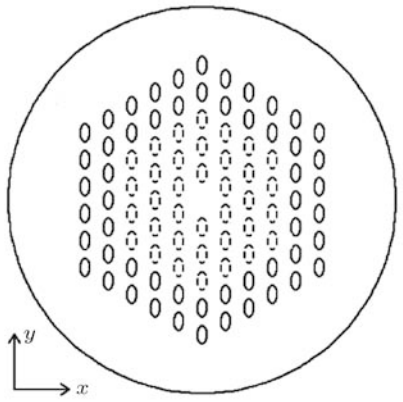


Fig. 2. Cross sectional schematic diagram of an MOF.

The changes of the SOPs in the MOF can be simulated with the following reference parameters. In the cross section, the value of PDL is about -0.0002 dB/m in x-axis direction, and about -0.14 dB/m in y-axis direction, so the parameters g_x and g_y were set to be $-0.001\times(1+d_x)$ and $-0.032\times(1+d_y)$, where d_x and d_y are small range random disturbances. The beat length of this MOF is about 0.4 $-$0.6 mm, $\Delta\beta$ is calculated to be distributed randomly from 2512 to 3768 rad/m, while k from 0.01 to 0.1. At first, every segment Δz was set to be 0.00005 m, then the evolvement tracks of SOPs on the Poincaré sphere are calculated for z from 0 to 0.5 m. Figure 3 shows the simulated tracks of the SOPs.

In Fig. 3, the solid symbols on the Poincaré sphere are the beginning SOPs of the SOP evolvement tracks, the consecutive small points built up the tracks and the hollow symbols are the end SOPs. One symbol stands for an SOP, circle, square, diamond, triangle, pentagram and hexagram for Stokes parameters $[1\ 1\ 0\ 0]^{\mathrm{T}}$, $[1\ 0\ 1\ 0]^{\mathrm{T}}$, $[1\ 0\ 0\ 1]^{\mathrm{T}}$, $[1\ -1\ 0\ 0]^{\mathrm{T}}$, $[1\ 0\ -1\ 0]^{\mathrm{T}}$ and $[1\ 0\ 0\ -1]^{\mathrm{T}}$, respectively. It is easy to find that the changes of the SOPs are not distinct on the Poincaré sphere for 5 m transmission length, some points are almost unmoved and the other points only vary along the longitudes.

Then the segment Δz was assigned to be 0.05 m, and the evolvement tracks of the SOPs on the Poincaré sphere for z from 0 to 500 m were simulated. Figure 4 is the simulated tracks of the SOPs, with (a) being a figure with all tracks, while (b) being the simplified figure which only contains the start and end points. The exact details of the SOP changes in the MOF can be obtained from the figures. The two pictures show that all the SOP evolvement tracks rotate along a same axis and end at the same point. It means that the SOP is constringed to a point from any location on the Poincaré sphere after enough long transmissions. The locations of the axis and the point are determined by the values of parameters in the Mueller matrix $\boldsymbol{M}$.

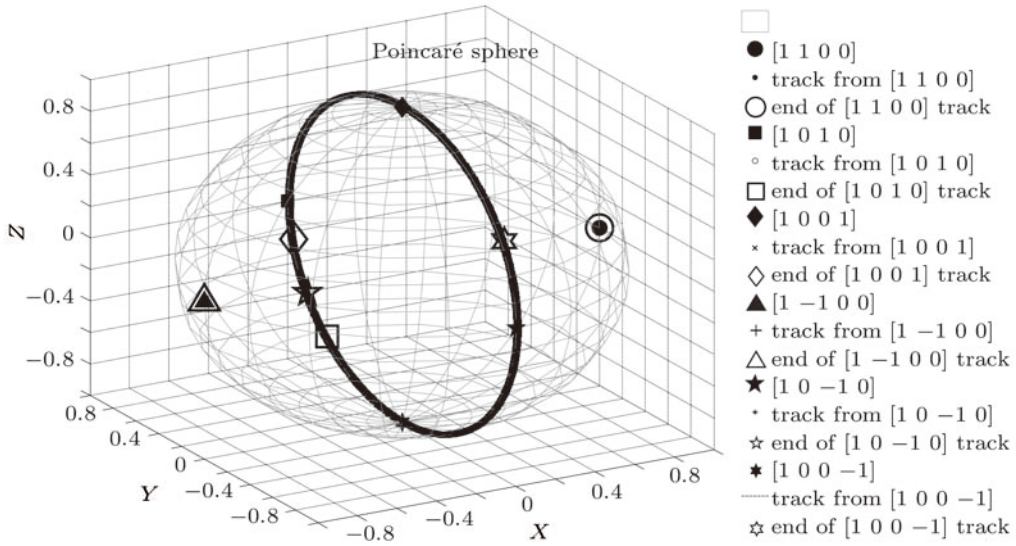


Fig. 3. Simulated tracks of the SOPs for z from 0 to 0.5 m.

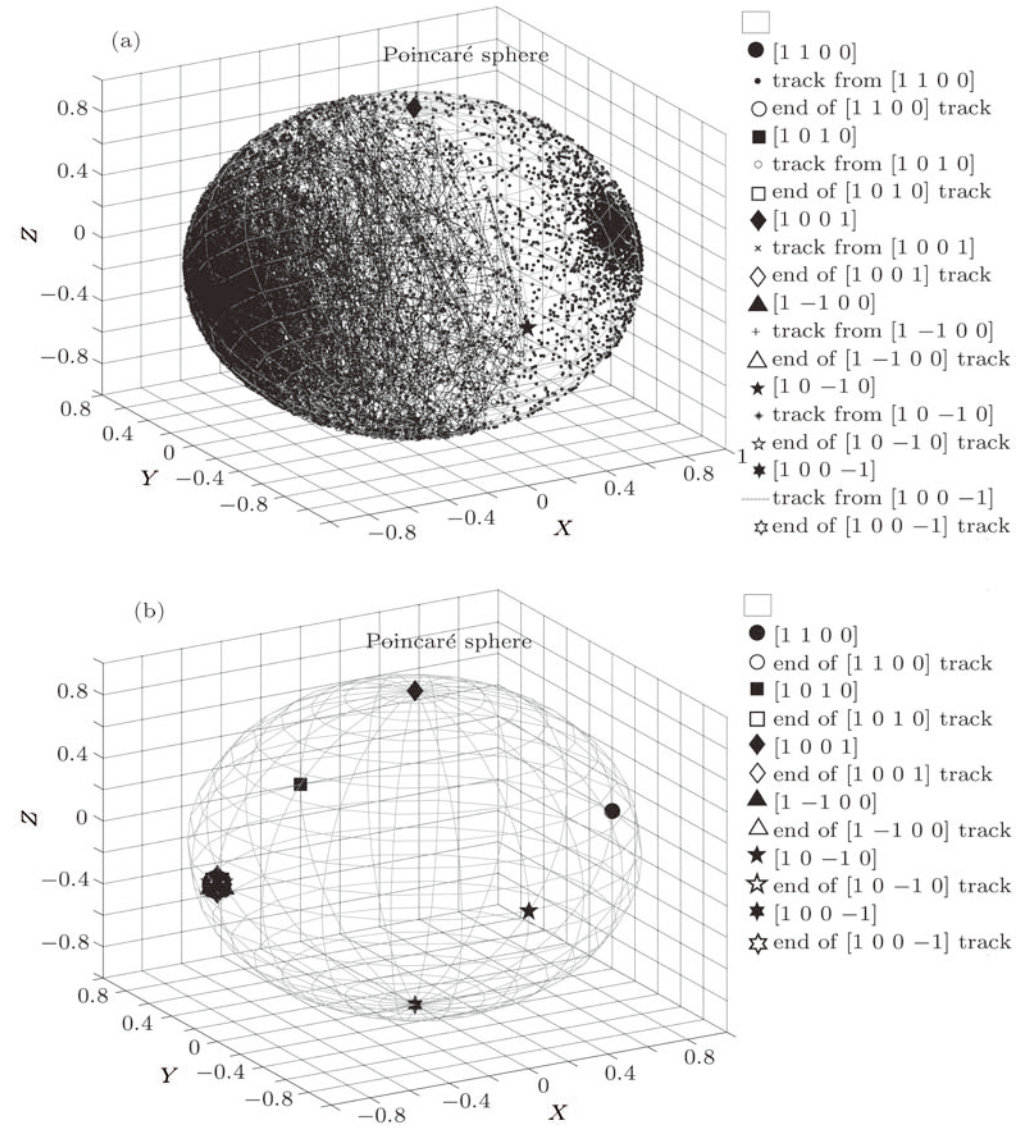


Fig. 4. Simulated tracks of the SOPs for z from 0 to 500 m: (a) the SOP tracks, (b) only the start and end points.

In a word, at a single wavelength, if all of the mode coupling coefficient k, propagation constants β_x and β_y, gain coefficients g_x and g_y are almost invariant, the phenomena of the SOP constringency is obvious after a sufficient transmission distance, and the point of SOP constringency and the distance can be calculated.

5. Conclusion

To our knowledge, we obtained the Mueller matrix with co-existence of birefringence-PDG-mode coupling at a single wavelength which was defined for the first time and can be used to investigate the changes of the SOPs optical fibers. The changes of the SOPs in a special MOF using the new Mueller matrix analysis were simulated and the hyperfine SOPs evolvement and the phenomena of SOP constringency for long transmission distance were obtained. The new Mueller matrix analysis can be used for studying the hyperfine changes of the SOPs and designing structures related to the SOPs in almost any optical fibers, especially for fibers which have microstructure.

References

[1] Sunnerud H, Xie C J, Karlsson M, Samuelsson R and Andrekson P A 2002 *J. Lightwave Technol.* **20** 368

[2] Erdogan A T, Demir A and Oktem T M 2008 *J. Lightwave Technol.* 26 1823

[3] Fu S N, Wu C Q and Shum P 2005 *Chin. Phys.* B **14** 1591

[4] Yan H and Li G F 2005 *Opt. Express* **13** 7527

[5] Kazovsky L G and Kalogerakis G 2006 *Proc. CLEO'2006*, Long Beach, CA, 2006 CMDD1

[6] Karbassian M M and Ghafouri-Shiraz H 2008 *J. Lightwave Technol.* **26** 3820

[7] McGeehan J E, Nezam S M R M, Saghari P, Izadpanah T H, Willner A E, Omrani R and Kumar P V 2004 *Proc. OFC'2004*, Los Angeles, CA, 2004 EF5

[8] Zhang C, Mori Y, Igarashi K and Kikuchi K 2008 *Proc.OFC/NFOEC'2008* San Diego, CA, 2008 PDP6

[9] Xiao L, Zhang W, Huang Y D and Peng J D 2008 *Chin. Phys.* B **17** 995

[10] Goldstein D 2003 Polarized Light edn. 2 (New York: Marcel Dekker Inc.) p. 31

[11] Shurcliff W A 1962 *Polarized Light* (Boston: Harvard University Press) p. 109

[12] Li Z Y, Wu C Q, Dong H, Shum P, Tian C Y and Zhao S 2008 *Opt. Express* **16** 3955

[13] Keiser G 2002 *Optical Fiber Communications* edn. 3 (Beijing: Higher Education Press) p. 122

[14] Dong H, Shum P, Yan M, Zhou J Q, Ning G X, Gong Y D and Wu C Q 2006 *Opt. Express* **14** 5067

[15] Dong H, Shum P, Gong Y D and Wu C Q 2007 *Opt. Lett.* **32** 2999

[16] Wu C Q 2005 *Theory of Optical Wave-Guide* edn. 2 (Beijing: Tsinghua University Press) p. 168

[17] Wu C Q and Dong H 2002 *J. Lightwave Technol.* **20** 1604